DEVELOPMENT OF A COMPACT PAYLOAD MECHANISM ENABLING CONTINUOUS MOTORIZED SENSOR HEAD ROTATION AND SIGNAL TRANSFER

Matthias Noeker [1, 2], Emiel Van Ransbeeck [3, 4], Özgür Karatekin [1] and Birgit Ritter [1]

[1] *Royal Observatory of Belgium, Ringlaan-3-Avenue Circulaire, 1180 Uccle (Brussels), Belgium*

E-mail: matthias.noeker@observatory.be

[2] *Université catholique de Louvain, Place de l'Université 1, 1348 Ottignies-Louvain-la-Neuve, Belgium*

[3] *VRE Consultancy, Dries 15, 1745 Mazenzele, Belgium*

[4] *Royal Belgian Institute for Space Aeronomy, Ringlaan-3-Avenue Circulaire, 1180 Ukkle (Brussels), Belgium)*

ABSTRACT

In this study, we present a mechanism enabling a continuous, non-restricted and bidirectional rotation of a sensor head for a scientific instrument. The rotation of the sensor head along-axis is done with a gear motor (i.e. a stepper motor with planetary gearbox) and a gear train. The target accommodation volume of the instrument is within only one CubeSat unit (1U = (10 cm)³), demanding an extremely compact design. The need of a rotating system for bias rejection and levelling for a gravimetric measurement for planetary exploration has triggered the development of such a mechanism at the Royal Observatory of Belgium. This mechanism forms part of the GRAvimeter for small Solar System bodies (GRASS). GRASS has been selected for the Juventas CubeSat that will attempt to land on the moonlet of the binary asteroid system, Didymos, within ESA's Hera mission.

1. INTRODUCTION

In the context of the GRASS instrument development for the Juventas deep-space CubeSat, as part of the ESA Hera mission, a space mechanism has been developed that enables continuous motorized sensor head rotation and signal transfer [1]. Such a mechanism is not only of avail for gravimetric measurements demanding levelling and bias rejection, but can likewise be used for instrument pointing or mechanical manipulation of the instrument, e.g. applying filters.

One instrument with a comparable working principle was the quasi-steady acceleration measurement (QSAM) instrument that modulated the acceleration measurements aboard spacecraft by turning the sensor by 180° [2]. This mechanism therefore only provided a restricted sensor head rotation capability. Only little information is known about the mechanism design, except that it used a stepper motor with an angular detector. Regarding pointing mechanisms, a wide range of solutions exists, however, generally in the context of antenna, thruster, or telescope pointing. We were not able to locate a space mechanism comparable to the here presented.

This paper presents the design, manufacturing and testing of the mechanism prototype that has been fully integrated and tested, and which has advanced to the gravimeter testing phase. Moreover, the requirements relevant to the mechanism design are listed (Section 2). The here presented compact mechanism prototype forms the basis of the GRASS flight model mechanism currently under development.

2. MECHANISM REQUIREMENTS

This Section presents and explains the requirements posed to the space mechanism development. Generally, the requirements are identical to the flight hardware, yet the constraints on volume/mass were defined less strict to allow mounting an experimental (larger) gravimeter sensor head.

2.1 Sensor head

Regarding the sensor head, i.e. the payload part to be rotated that performs the measurement, there are three main requirements:

- REQ-001: The mechanism shall enable continuous, bi-directional and unrestricted rotation of the sensor head, with a safety factor of at least 3 for the torque.
- REQ-002: The mechanism shall drive the sensor head volume (solid of revolution) of diameter 33.5 mm and length 89.9 mm.
- REQ-003: The mechanical noise induced to the sensor head shall be minimized.

With REQ-002 addressing the sensor head, no numerical volume and mass constraints were formulated for the instrument mechanism, while the target accommodation volume of the flight mechanism is one CubeSat unit (1U = (10 cm)³). Yet, the here presented design is, within REQ-002, optimized for a lightweight and compact design.

2.2 Rotor-Stator Electric Contact

With respect to the rotating sensor head, the following requirement has been formulated:

- REQ-004: The mechanism shall provide continuous, uninterrupted electrical connection between the instrument back-end electronics and sensor front-end electronics.

Here, it is noted that the electrical connection (REQ-004) is also influenced by the sensor head requirement REQ-001.

2.3 Angular position measurement

Concerning the sensor head measurement, the final requirement reads:

- REQ-005: The mechanism shall provide the angular position and rotation direction of the sensor head at least once per revolution.

In case of an undesired loss of power or reboot, the instrument might lose knowledge of the sensor head position. Performing a "homing" at least once per turn allows regaining the angular position, provided the rotation can be recorded. Due to REQ-001, this requirement is not driven to avoid crashing the instrument, but rather needed for instrument operations and to supplement the science measurement.

3. MECHANISM DESIGN AND COMPONENTS SELECTION

Based on the requirements formulated in the previous Section, the mechanism can be grouped in three fields, sensor head rotation (Section 3.1), rotor-stator electric contact (Section 3.2), and angular position measurement (Section 3.3). Using this, the mechanism architecture is introduced in Section 3.4.
Generally, all components that are presented in this Section are provided as "space-grade" or "space-versions", but they are not space-qualified individually by the manufacturer. For the here presented mechanism, it would be more practical to space-qualify the assembly on *mechanism*-level, rather than the individual components. For this prototype, however, no full space-qualification has yet been performed. Rather, the flight model design, currently under development, will be used for qualification tests.

The drivers of the component and material selection include torque requirements, behavior with temperature (operational temperatures and material properties) and long-term storage capabilities.

3.1 Sensor head rotation

This Section discusses the arrangement of the motor to the sensor head as well as the transmission of the motor torque.

For the arrangement, there are three main options: parallel, orthogonal, and in-line arrangement between motor and sensor head; where only the latter allows a direct connection between motor shaft and sensor head without gears. A pair of gear wheels, however, can also serve to protect the motor output shaft during vibration and shock, partially decoupling these two components.

Depending on the allocated payload volume and form factor, options might have to be discarded directly. The in-line option minimizes the instruments cross-section, while the length is maximized. On the contrary, the parallel solution increases the instrument cross-section in one direction, while it minimizes the instrument overall length. Lastly, bevel gears with orthogonal axes between motor shaft and sensor rotation axis provides the intermediate solution: The instrument length is increased by the larger of motor and motor-gear diameter. The cross section becomes larger in one direction by the excess of motor length sticking out of the diameter of the solid of rotation of the sensor head.

With the instrument length being the most limiting factor in our application (100 mm), the in-parallel solution was selected and will be presented, noting that a different form factor of the mechanism can be realized by changing this configuration. In order to satisfy REQ-003, we concentrated on achieving a very good alignment between motor and sensor rotation axes. For this, we machine the mechanism housing in a single piece, containing the motor mounting hole together with the bearing holes for the sensor head.

Ideally, the holes for the bearings are drilled first and then measured precisely with a 3D coordinate-measuring machine. Only then, the motor hole should be drilled. This ensures not only best alignment between the motor axis and the sensor head axis, but also the precision of the distance between these two. This solution requires to mount the gear-motor with the assembled motor gear wheel in one piece, demanding a mounting hole with the diameter of the latter as shown in Figure 1. Note that in this application, we have increased the nominal distance between the motor and the sensor head axes from the nominal 25 mm to $d = 25^{+0.03}_{+0.02}$ in order to avoid blocking of the mechanism due to thermal expansion.

In the following, the selection of the gear motor, the gear train and the bearings is described.

While studying various possible motors, a strong emphasis was laid upon both mass and volume. We finally identified an extremely compact solution being the CoograDrive® Space 10 mm - Type 6 from Micromo-

tion GmbH. The drive consist of a stepper motor (20 steps per revolution, 2 Volt) and a low-backlash CoograDrive® planetary gearbox (reduction ratio 80:1). The delivered torque (Section 5.1) is 15 mNm at a low mass of ca. 13 gram. The total length is 36.15 mm and the diameter of 10 mm is only exceeded for the mounting holes, thus the assembly in the single piece motor mount works without restriction. One concern regarding deep-space exploration was the creep of the lubricant, both during pre-launch ground-storage and deep-space cruise phase. The applied lubricant for the gearbox and the motor bearing are Braycote601EF and Braycote815Z, respectively. To mitigate creep, a modification of the product is applied using a creep barrier based on epilamiziation, applied in the area of output bearing, gear component set and motor bearing. Moreover, it is suggested to exercise the mechanism regularly, (ideally once a month, at least once per half-year), during both ground storage and cruise to further mitigate the lubricant creep.

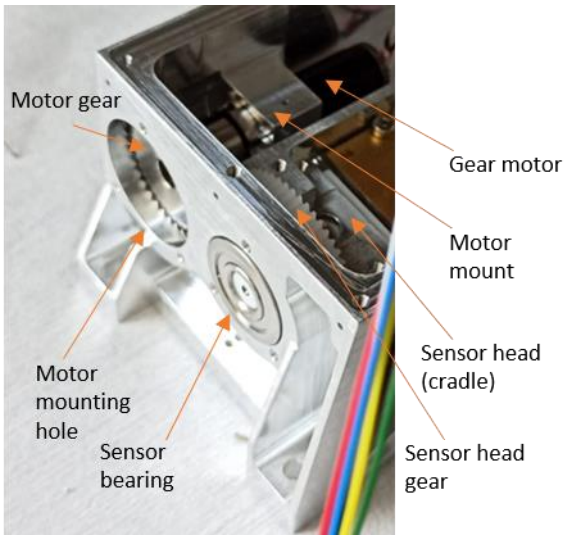

Figure 1. Single-piece housing mounting sensor bearings and motor allowing for a very good alignment control. The dedicated mounting hole for the motor with its gear is covered after integration.

The sensor head is designed as a cradle, i.e. a continuous shaft with the central part allowing mounting of the payload, e.g. front-end electronics, sensors etc. based on the application. This cradle is mounted and rotated using two flanged bearings. Again, like for the motor it is desired to have the bearing holes machined in the same piece, allowing very good alignment of the bearings and therefore reducing a possible source of mechanical noise. To compensate for axial play, especially for differential thermal expansion between structure and sensor-mounting shaft, a wave washer will be used for one bearing. The flange in combination with bearing covers (also for electromagnetic compatibility (EMC)) maintains the axial position of the parts.

For the application in space, the requirements to the bearings include low torque (Section 5.1), a large operational temperature (Section 5.3), no outgassing, and a lubricant that does not require sealing, to avoid creeping losses. The BarTemp bearings from Barden UK satisfy all these requirements, where the bearing is self-lubricating. The selected bearings are SRF4SS, where SS indicates shielded. These bearings have extensive heritage in space, in one case for example having performed 10^{10} revolutions on orbit [3]. According to [3], the self-lubrication from the bearing cage, however, requires that incremental rotation is in the order of at least 30° to provide a film on the balls, which can also be realized by the above mentioned maintenance exercise of the mechanism. Depending on the application, this problem will require further testing, especially if the mechanism is not design for continuous, but rather incremental rotation (e.g. pointing). In this case, the operation plan could include 1 to 3 rotations prior to such incremental movement to allow for initial self-lubrication of the self-lubricating bearing.

As it is common practice in space mechanism development, the gear train consists of one metallic (stainless steel) and one non-metallic (Delrin) gear wheel, to avoid cold welding between the moving parts. Obviously, the axis distance between sensor and motor is driven by the combined nominal gear radii. For the in-parallel motor alignment, this dimension is a limiting factor on the sensor head diameter. Generally, to increase the delivered motor torque, the gear ratio i should be sized such that it is not smaller than i=1, ideally it will be i>1, increasing the available torque while reducing the rotation speed inversely. As stated above, mechanism jamming due to thermal expansion is avoided by increasing the axes distance at little cost of the gear efficiency and backlash (Section 5.2). We selected gear wheels from HPC Europe with module 0.5. The larger Delrin wheel has a reference circle diameter d_P = 30 mm (60 teeth) and is attached to the sensor head. The stainless steel wheel has 40 teeth at d_P=20 mm and is driven by the motor. The resulting gear ratio is therefore

$$i = \frac{30mm}{20mm} = \frac{60}{40} = 1.5. \qquad (1)$$

Our gear combination yields some play (Section 5.2), which, in our application with (generally) unidirectional rotation and position measurement is acceptable; this decoupling is even desired to protect the fine gear motor from damage in vibration and shock.

3.2. Rotor-stator electric contact

Clearly, using the rotary sensor can only be achieved by a reliable, yet not constraining connection from the measuring sensor to the stationary part of the instrument. Generally, this realizes a connection from the front-end electronics within the sensor head to the back-

end electronics of the instrument. Since both data communication and power need to be transmitted, we disregard wireless solutions and present two options allowing direct connections.

Firstly, a flex cable winded around the sensor rotation axis allows a quasi-undisturbed data and power transmission. The winding of the flex cable, however, implies several disadvantages: The rotation of the sensor head will always be constraint and therefore, the rotation direction must be inverted regularly. We estimated that this option would not allow more than 3 to 5 rotations. Additionally, the winding of the flex cable with constantly changing bending radius will result in a constantly changing torque on the drive system (Section 5.1), potentially inducing additional mechanical noise to the measurement. With requirements on the bending radius, the outer diameter of this solution would have exceeded the sensor head diameter. Lastly, an absolute homing mechanism, e.g. for unexpected loss of positional knowledge (loss of power, reboot of system, safe mode etc.) will be required.

The alternative solution that we selected is a slip ring. Here, contact from the rotary part is realized with circular "runways" mounted over one part of the rotating sensor shaft that are in contacts with stationary "fingers", or brushes. Each power/data line has one of the contact areas and therefore the number of lines can generally be adapted to the needs (with some increase in length). These outer contacts "slip" over the rotating runways and the contacts should be redundant, i.e. with two fingers per line as visible in Figure 1. Generally, we considered two types of slip rings, a separable and encapsulated one. While the separable inner ring is mounted over the turning shaft, the encapsulated version is added in-line as an extension to the cradle. For integration reasons, we have selected the separable version.

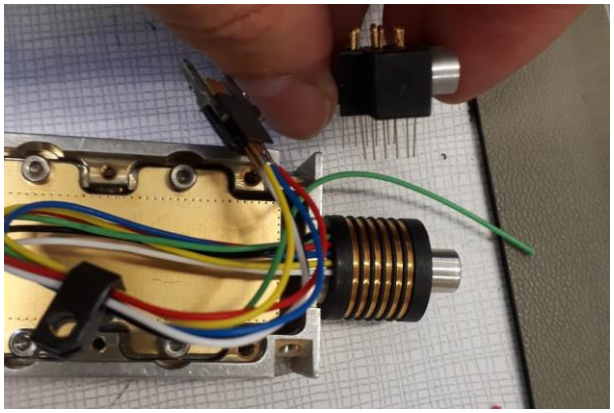

Figure 2. Separable slip ring with runways mounted on the cradle shaft for integration. The stator parts can be added after integration of the cradle and rotated in the final screw fixation position.

While this solution solves the above listed problems with the flex cable, some other constraints emerge: Regarding the signal transmission, there will always be some noise induced, more so during rotation, disqualifying the noise-free transmission of analogue signals. The measurement therefore requires front-end electronics creating a digital signal to be passed. Other than the motor, the slip ring obviously cannot be aligned in parallel, thus adding to the overall instrument length and, for a defined max. instrument length, reducing the length available to the sensor.

Regarding alignment, the encapsulated slip ring is a self-contained subsystem with the alignment quality depending on the purchased component. For the separable slip ring, this alignment is controlled by the quality of assemblage. With the housing made in one piece also mounting the slip ring "fingers", a very good alignment is achieved in the here presented mechanism.

Regarding the component selection, Moflon Technology Co., Ltd. provides an aerospace version of their slip rings. Here, for the separable part we have selected the MSP1069 where the "9" denotes the "high-end quality-version". This slip ring has six lines for signal or current up to 2A. The nominal torque is only 5 mNm and was found to be even lower than 3.1 mNm (Section 5.1). Finding an extremely compact component with such low torque was one of the main challenges when selecting a slip ring.

3.3. Angular position measurement

Rotating the sensor head will generally require to record the phase of the rotation along with the measurement being taken. For this, there are different possibilities both giving the relative and absolute position. Due to REQ-001 and REQ-005, absolute position measurement is not required here to avoid jamming the stator-rotor connection. Due to the unconstrained rotation, relative knowledge of the position is therefore sufficient. For this, a "homing" is performed at least once per revolution uniquely giving the position of the sensor. From there, the revolution made is measured, e.g. by counting the steps of a stepper motor and subsequently verifying the counted steps with the next recorded revolution.

Overall, we have studied four options for position measurement of the rotating sensor head:

- Reed switch
- Mechanical switch
- Encoder in motor
- Optical switch

The reed switches, triggered by a small magnet within the rotating sensor gave unsatisfactory results, with partially more than one triggering of the reed switches, making the readings unusable. The mechanical switch

with additional moving parts and added torque requirements was disregarded due to these drawback and their added complexity. One very interesting option offered by the motor supplier is to equip the gear-motor directly with an encoder, added to a gear motor. In this case, the length were to be increased by ca. 10 mm. While the proposed 12-bit absolute single turn encoder (4.096 steps per revolution) can be used in high-vacuum, deployment in deep-space will require further investigation. We had to disregard this option as this solution does not work with a stepper motor, but rather a brushless DC motor, requiring a nominal voltage of 6 V rather than 2 V of the used solution.

Finally, we have selected two optical switches that are interrupted with a "fin" (Figure 3). The optical sensor chosen is the Photomicrosensor (Transmissive) EE-SX1018 sensor from Omron. Placing two sensors behind each other allows to determine the direction of rotation.

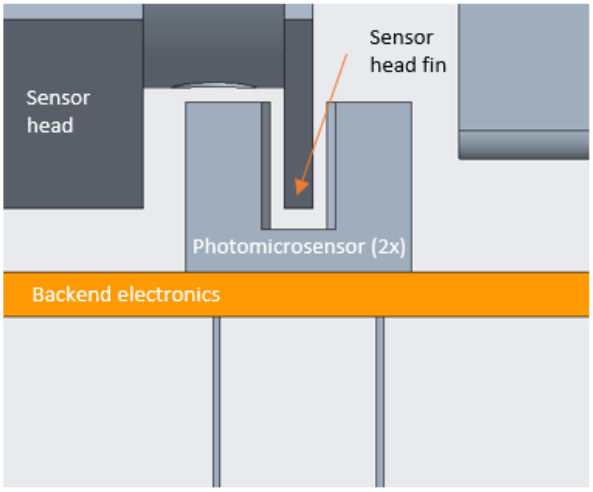

Figure 3. Sensor head fin interrupting the two photomicrosensors (transmissive), directly mounted behind each other on the back-end electronics (shown in orange).

This contactless solution was tested successfully and additionally provides redundancy in the positioning, while a single sensor cannot determine the direction of rotation, which, however, will generally be known from the motor controller. Regarding the distance between the rotation axis and the backend electronics, the fin design can be adapted according to the required distance.

3.4 Mechanism Architecture

The previous three Sections have presented the three main building blocks of the here presented mechanism. In summary, the sensor head is rotated by means of a gear motor and a gear train. Continuous power and signal transmission between the rotor and stator is realized by a separable slip ring and the attitude of the rotary sensor can be recovered once per turn by triggering the optical sensors. The global mechanism architecture combines these three elements. For this, the single-piece housing is a key element, as it mounts the different subassemblies. As stated above, the machining in one piece allows very good alignment of the different components, ensuring very good torque transmission while minimizing mechanical noise. Figure 4 shows the annotated CAD model with the main elements.

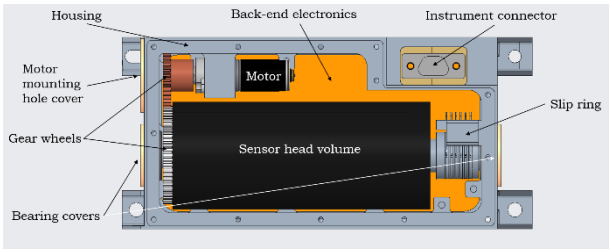

Figure 4. Working principle of payload mechanism to rotate and position any sensor head fitting within the black cylinder with diameter 33.5 mm and height of 80.9 mm.

The design accounts for assemblage to introduce the cradle shaft as a whole; likewise all other components can be assembled without problem. For EMC reasons, the payload mechanism was designed to be fully enclosed by different covers. The bearing covers also served as axial fixation of the parts, and the motor mounting hole was covered with a similar cover. The two large covers, top and bottom, enclose the box-design of the housing.

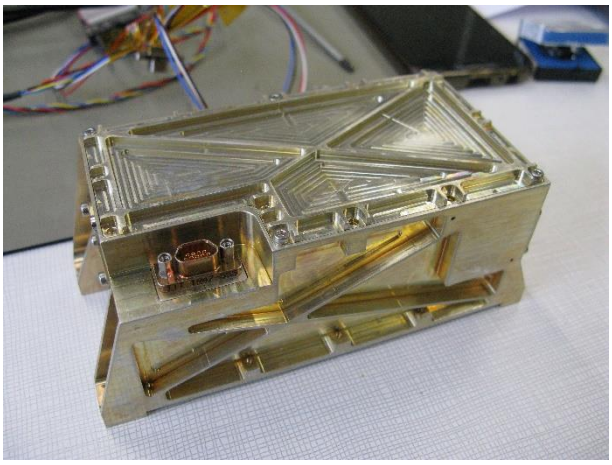

Figure 5. Mechanism housing with pockets and T-shaped cross ribs for an optimized mass budget and best structural stability.

Moreover, the housing has a larger hole to pass the (prewired) instrument connector coming from the backend PCB from the inside out. Two U-shaped brackets are then place between the connector and housing to close-off the housing here and allow fixation of the connector.

The aluminum housing and main (top) cover was optimized with respect to the mass and structural stability using pockets and T-shaped cross-ribs as visible in Figure 5. The total mass of the instrument is 288.3 gram, of which ca. 74 gram can be attributed to the application-dependent sensor head. Based on the application, the mass of the backend electronics and harnessing will vary.

The overall enclosing volume, including all mounting brackets is 129 x 60 x 52 mm³, still exceeds the target accommodation one CubeSat unit (1U = (10 cm)³) by 29 mm in length, while the flight model mechanism currently under development will meet this requirement. The bottom and two sides supplementary to Figures 1 and 5 are shown in Figure 6.

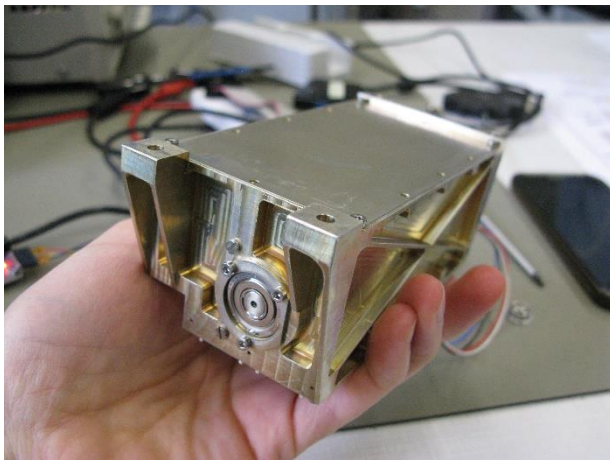

Figure 6. Bottom view of enclosed instrument with bottom cover and mounting interface. Supplementary to Figures 1 and 5, the mass optimization has been performed on all housing sidewalls.

5. MECHANISM TEST AND PERFORMANCE

In this Section, we present different tests and analysis regarding the mechanism performance. For this, a torque measurement has been performed (Section 5.1), the pointing accuracy is assessed (Section 5.2), the expected thermal operational range is listed (Section 5.3), and the lifetime and max. rotation speed is analyzed in Section 5.4.

5.1 Torque measurement

The nominal torque of the Micromotion motor is 15 mNm. In order to test if this is sufficient for the here presented mechanism (REQ-001), we employed a combination of a test and analysis.

Generally, the overall torque to be overcome is composed of the following contributions:

- Rotate moment of inertia of sensor head
- Bearings (2x) starting torque
- Slip ring starting torque
- Gear wheels friction (gear efficiency)

The starting torque of the first three contributions was measured with a simple test setup (Figure 7). In absence of the final sensor head, it is possible to compute the moment of inertia of the senor head CAD model and use a cylinder with equivalent moment of inertia. For the test, we used the gravimeter sensor head with a moment of inertia I_{XX} = 6.259 kg mm². Additionally to the moment of inertia, a good balance of the sensor head is required, that is represented by a center of gravity (CoG) very close to the rotation axis, which was the case for the used sensor head: the assembled sensor head has a CoG at only 0.0270 mm away from the rotation axis.

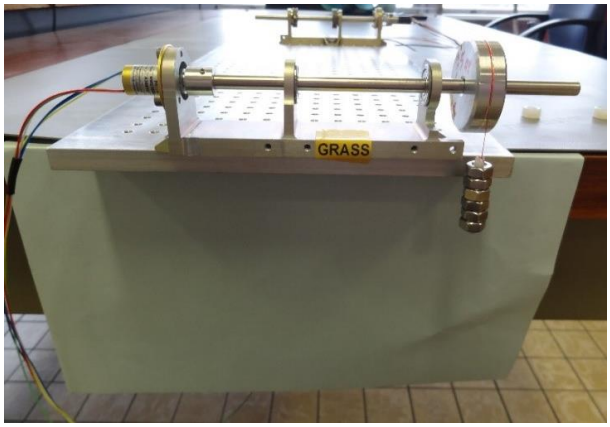

Figure 7. Torque measurement test setup with equivalent moment of inertia disc. Note that here the encapsulated Moflon slip ring was used for the test.

Torque M_T is the cross product of radius R and force F

$$M_T = R \times F \qquad (2)$$

so the starting torque is measured by dispending a mass on a string at the disc radius of 20 mm. Incrementally increasing the suspended mass, the holding torque was overcome at a mass of 15.8 gram at radius of 20 mm. Therefore, the starting torque is calculated as

$$M_{T,start} = 0.0158\,\text{kg} \cdot 9.81\,\frac{\text{m}}{\text{s}^2} \cdot\ 0.02\,\text{m}\ = 3.1\,\text{mNm}. \qquad (3)$$

This value is clearly below the nominal torque of the slip ring alone (5 mNm), where we used the encapsulated equivalent slip ring in the test. Following this, the gear efficiency is assumed as $\eta = 0.9$ and the gear ratio that is here $i = 1.5$. The minimum nominal torque for the gear motor is therefore

$$M_{T,min} = \frac{M_{T,start}}{i \cdot \eta} = 2.3 \text{ mNm.} \quad (4)$$

With the nominal torque of the motor being 15 mNm, the safety factor S can be computed as

$$S = \frac{M_{T,nom}}{M_{T,min}} = 6.5 \quad (5)$$

where we demanded a minimum of 3 for space applications in REQ-001.

5.2. Pointing Accuracy and Backlash

The error in pointing the sensor results from the combination of the backlash of the motor output shaft and the gear train. The motor has a theoretical backlash of 20 arcmin as stated by the supplier. The combined play of motor and gear train was measured to be better than 2.3°. For uni-directional rotation for signal modulation, combined with the position knowledge (Section 3.3), this was acceptable for the specific application. For critical pointing requirements, however, backlash mitigation measures, including a zero-backlash gear train need to be implemented, generally at the cost of required torque (Section 5.1). In this case, the protection of the motor-gear would be lost due to the zero-backlash gears. Here, it is possible to replace the selected drive by another Micromotion product that includes a slip clutch for protection of the gear motor interior.

Additionally, the axis distance was increased above the nominal for thermal reasons that increased the play (Section 3.1). Lastly, the used Delrin gear was molded, replacement by a machined high-precision gear (as used for the other, stainless steel gear) is foreseen for the ongoing development and the flight hardware.

5.3. Thermal Operational Range

The thermal constraints on the mechanism are driven by the three purchase components gear motor, bearings, and slip ring; the operational temperature (T_{op}) range is summarized in Table 1.

Table 1. Minimum and maximum operating temperature of relevant mechanism components, determining the range for the overall mechanism, as provided in the data sheets.

Component	$T_{op, min}$	$T_{op, max}$
Slip ring	-30 °C	+80 °C
Bearings	-200 °C	+100 °C
Gear motor	-10 °C	+70 °C
Mechanism	**-10 °C**	**+70 °C**

The resulting temperature range of the mechanism is therefore from -10 °C to +70 °C. The viscosity of the lubricant drives the cold limitation of the gear motor. In cases where this is critical, the stepper motor can be kept powered on continuously, or a "pre-heating" can be implemented in the payload operations by powering the windings of the motor without turning the motor.

Additionally to the listed components, we have analyzed the thermal expansion effect on the axis of the gear train. While the cold case is not a problem, the warm case, i.e. 50 degrees above the machining reference temperature of 20°C (ISO 1) [4] could pose a problem. In the hot case, the two gear wheels will expand which could block the mechanism, however, the aluminum housing, defining the axis distance, likewise expands, avoiding any problems here.

5.4 Lifetime and maximum rotation speed

The lifetime of the mechanism is driven by the shortest lifetime of the three sub-components. Also, the maximum rotation speed is given by the slowest maximum rotation speed of slip ring, motor and bearings (Table 2). The bearings with basic dynamical load rating C = 694 N and static radial capacity C_0 = 120 N are the least-limiting components.

Table 2. Overview of the mechanism lifetime and maximum rotation speed determined by the three relevant sub-components. Numbers provided by the manufacturer, or calculated based on data sheet information (lifetime bearings).

Component	Lifetime [rev.]	Max. rot. speed [RPM]
Slip ring	100 million	1000
Bearings	>300 million (L_{10})	9450
Gear motor	300 million	262.5
Mechanism	**100 million**	**262.5**

The testing of the mechanism was, however, only done at very low speeds, i.e. less than 10 RPM and at stepwise (pointing) rotation. For high-rotation speeds, approaching the maximum rotation speed, or for experiments with extensive life time, further testing is required.

6. DISCUSSION AND FUTURE DEVELOPMENT

The presented mechanism is compliant with all laid-out requirements. It allows continuous motorized sensor head rotation and signal transfer for various possible applications. The single-axis instrument is developed only using space-qualified materials and space-version components, but a full space-qualification campaign has not yet been performed for this mechanism. Trade-offs during the mechanism development were performed, allowing to re-evaluate the decisions made for possible different requirements and/or constraints.

The compact design and overall mass is well suited for space exploration missions. Likewise, the performance numbers regarding lifetime and torque provide excellent results. The temperature range, pointing and operational speed provide figures well suitable for most use cases. The instrument, being fully enclosed in the housing with its covers, satisfies EMC requirements.

Regarding the development of the flight model mechanism, the here presented work forms the foundation of the ongoing development. The presented performance and results allow to maintain the general mechanism principle, while the target accommodation volume of one CubeSat Unit (1U = (10 cm)³) for two axes will require an even more, extremely-compact design. This study has shown that this will demand not only a miniaturization of the mechanism, but also the sensor head and, in the context of the GRASS gravimeter, the sensing element.

7. CONCLUSIONS

Here we present a space mechanism concept enabling a payload sensor to be rotated along its long axis continuously and bi-directionally; also enabling precise pointing of the sensor. Following a qualitative introduction of the necessary building blocks, the technical implementation is discussed. Based on this, the performance of the mechanism regarding torque, pointing accuracy, thermal constraints, and lifetime and maximum rotation speed is assessed. While this mechanism was developed as part of the GRASS gravimeter, the mechanism provides a manifold of possible future applications within our Solar System.

ACKNOWLEDGEMENT

We are grateful for the support of the Royal Belgian Institute for Space Aeronomy (BISA) technicians and engineers helping in manufacturing the presented mechanism.
The authors acknowledge funding support from the PRODEX program managed by the European Space Agency (ESA) with help of the Belgian Science Policy Office (BELSPO) and from the European Union's Horizon 2020 research and innovation program within the NEO-MAPP project.
M.N. acknowledges funding from the Foundation of German Business (sdw) and the Royal Observatory of Belgium (ROB) PhD grants.

REFERENCES

1. Karatekin, Özgür, et al. (2021). Surface gravimetry on Dimorphos. No. EGU21-15901. *Copernicus Meetings.*
2. Hamacher, H., R. Jilg, and B. Feuerbacher (1991). QSAM-A measurement system to detect quasi-steady accelerations aboard a spacecraft. *Acta Astronautica* 24: 243-249.
3. Hadley, H. (1980). in *14th Aerospace Mechanisms Symposium: Proceedings of a Symposium held at NASA Langley Research Center, Hampton, Virginia, May 1-2, 1980, vol. 2127 (NASA Scientific and Technical Information Office), vol. 2127, p. 101*.
4. Doiron, T. (2007). 20 C—A Short History of the Standard Reference Temperature for Industrial Dimensional Measurements. *Journal of research of the National Institute of Standards and Technology*, *112*(1), 1.